

PDF hosted at the Radboud Repository of the Radboud University Nijmegen

The following full text is a publisher's version.

For additional information about this publication click this link.

<http://hdl.handle.net/2066/112830>

Please be advised that this information was generated on 2021-10-28 and may be subject to change.

Invited paper

Metamagnetic transitions in the heavy-fermion system $U(\text{Pt}, \text{Pd})_3$

J.J.M. Franse^a, H.P. van der Meulen^a, A.A. Menovsky^a, A. de Visser^a,
J.A.A.J. Perenboom^b and H. van Kempen^b

^a *Natuurkundig Laboratorium der Universiteit van Amsterdam, Valckenierstraat 65, 1018 XE Amsterdam, The Netherlands*

^b *High Field Magnet Laboratory, University of Nijmegen, Toernooiveld, 6525 ED Nijmegen, The Netherlands*

High-field magnetisation measurements on single-crystalline samples of the heavy-fermion system $U(\text{Pt}_{1-x}\text{Pd}_x)_3$, reveal metamagnetic-type of transitions in the liquid-helium temperature region for Pd concentrations with x -values below 0.1 and field directions perpendicular to the hexagonal axis. These transitions are considered to reflect the suppression of short-range antiferromagnetic inter-site correlations and have further been investigated in specific-heat experiments with applied magnetic fields up to 24.5 T. For the compound with a Pd content equivalent with $x = 0.05$, in addition long-range antiferromagnetic order is found below 6 K. This long-range order is signalled in the specific heat at zero field by a sharp peak near 6 K. For magnetic fields applied perpendicular to the hexagonal axis, this peak shifts to lower temperatures with increasing field and seems to disappear for field values around 12 T, the field where the metamagnetic transition in the magnetisation experiments is observed. By combining the magnetisation and specific-heat data, magnetic phase diagrams have been constructed for the studied compounds.

1. Introduction

Shortly after the discovery of UPt_3 as a heavy-fermion compound [1,2], experiments were carried out in order to investigate the effect of substitutions on the uranium and platinum sublattices with respect to the anomalous low-temperature properties. Substitutions with Pd [3,4] and Th [5–7] immediately revealed additional ordering phenomena. So far, these substitution effects have most extensively been studied for the $U(\text{Pt}, \text{Pd})_3$ system and have led to the construction of a complex phase diagram in which superconductivity and long-range antiferromagnetic order occur besides spin-fluctuation and Kondo phenomena [8]. Some characteristic features of this phase diagram are: $U(\text{Pt}, \text{Pd})_3$ compounds up to 10 at% Pd fall into the class of heavy-fermion systems; superconductivity is easily depressed and compounds containing 0.5 at% Pd or more are no longer superconducting; long-range antiferromagnetic order is observed at higher Pd contents (2, 5 and 7 at% Pd) with a maximal value for T_N of 5.8 K for the 5 at% Pd compound; at further increasing the Pd content, the long-range antiferromagnetism becomes weaker and for the 10 at% Pd alloy hardly any sign of magnetic order is left. In this respect it is worth to mention that a really sharp transition in the specific heat is found for the 5 at% Pd alloy only. For the 7 at% Pd alloy and for the 2 at% Pd alloy in particular, the transition width is much broader in temperature and certainly less pronounced. Neutron experiments have revealed a magnetic moment per uranium atom of $0.6\mu_B$, approximately for the 5 at% Pd alloy with the moments

pointing along the crystallographic b -axis in the hexagonal plane [9]. Low-temperature resistivity measurements [10] performed on the same series of compounds reveal a strong increase with increasing Pd content and a continuous transition from a spin-fluctuation to a Kondo-type of resistivity behaviour. Susceptibility measurements as well as high-field magnetization measurements on single-crystalline $U(\text{Pt}, \text{Pd})_3$ compounds at 4.2 K show metamagnetic types of transitions for field directions perpendicular to the hexagonal axis [11]. The transition field is shifted to lower field values for increasing Pd content and approaches zero field for the 10 at% Pd alloy. Low-field susceptibility measurements confirm this trend by showing that the temperature at which the susceptibility develops its maximum, shifts from 18 K for pure UPt_3 to zero temperature at increasing the Pd content up to 10 at% Pd. These results are summarised in figs. 1–3. Similar results were reported for Th substitutions on the uranium sites [12]. Most remarkable is that antiferromagnetism is again best developed for a thorium content of 5 at%. Other 5 at% substitutions like Ce and Y on the uranium site or Rh, Os and Ir on the platinum site did not show these large effects on the low-temperature resistivity nor indicated magnetic order around 6 K. Apart from the long-range antiferromagnetic order that clearly shows up in the specific heat of the 5 at% Pd and Th compounds, weak antiferromagnetism with moments per uranium atom of the order of $0.02\mu_B$ has been observed in neutron experiments on some UPt_3 samples [13,14]. Similar neutron experiments on the Pd substituted alloys have not yet been performed.

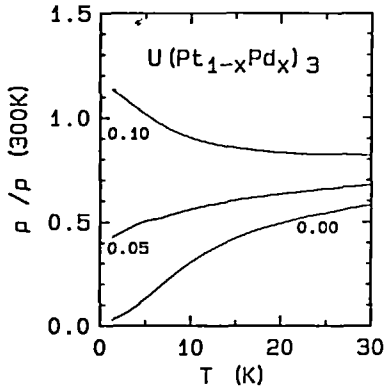


Fig. 1. Resistivity data for polycrystalline $U(Pt_{1-x}Pd_x)_3$ compounds in a plot of $\rho(T)/\rho(300\text{ K})$ vs. T ; the different curves are indicated by the corresponding x -values.

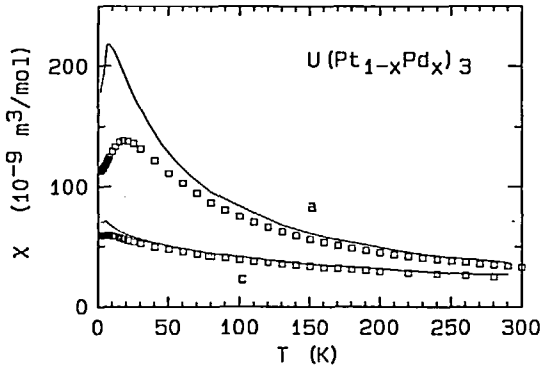


Fig. 2. Temperature dependence of the magnetic susceptibility of UPt_3 (full curves) and $U(Pt_{0.95}Pd_{0.05})_3$ (\square) along different crystallographic directions.

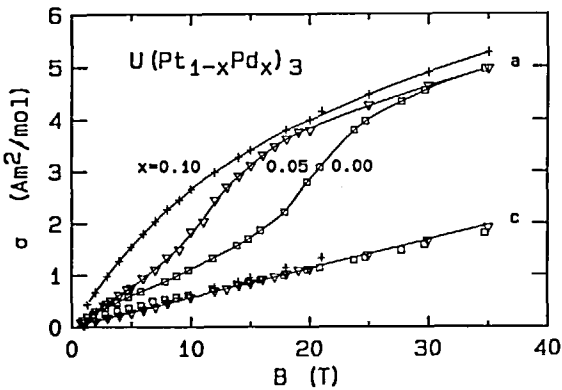


Fig. 3. High-field magnetization data for single-crystalline $U(Pt_{1-x}Pd_x)_3$ compounds for field directions parallel and perpendicular to the hexagonal c -axis; $x = 0.00$ (\square), $x = 0.05$ (∇), $x = 0.10$ ($+$).

2. Experimental

Specific heat measurements were carried out on single-crystalline samples of cubic shape ($5 \times 5 \times 5 \text{ mm}^3$) that were cut out by spark erosion of cylindrical batches grown by the Czochralski method in a tri-arc furnace. Susceptibility, resistivity and high-field magnetization measurements have been performed on different samples, in some cases out of the same batches. The cubic samples of UPt_3 and $U(Pt_{0.95}Pd_{0.05})_3$ have been used in thermal expansion measurements as well. The high-field specific-heat data of UPt_3 have been published before [15,16]. The results for $U(Pt_{0.95}Pd_{0.05})_3$ will be published elsewhere more extensively, the data for $U(Pt_{0.90}Pd_{0.10})_3$ are preliminary results. The specific-heat measurements are carried out at the Nijmegen High Magnetic Field Laboratory in a Bitter-type of coil for fields up to 20 T and in a hybrid system (superconducting magnet 8 T, Bitter coil 17 T) for fields up to 24.5 T. Experiments were performed in an adiabatic way with a sapphire sample holder equipped with a ruthenium-oxide thermometer and a nickel-chromium film as a heater.

3. Results and discussion

The composition dependence of the specific heat in the $U(Pt, Pd)_3$ system is illustrated in fig. 4. The compounds with 0, 5 and 10 at% Pd all have large c/T values down to the lowest temperatures with the largest value at 1.3 K for the 10 at% Pd compound. Antiferromagnetism in the 5 at% Pd alloy is signalled by the pronounced peak just below 6 K. Most remarkable, as noticed several times before, are the large c/T values for the 5 at% Pd alloy below the magnetic ordering temperature. Apparently, long-range antiferromagnetic

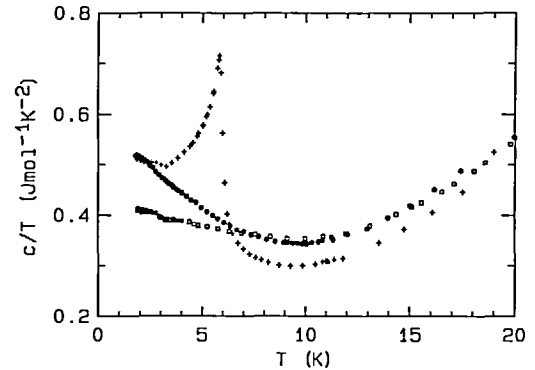


Fig. 4. Specific-heat data at zero field for $U(Pt_{1-x}Pd_x)_3$ compounds in a plot of c/T vs. T ; $x = 0.00$ (\square), $x = 0.05$ ($+$), $x = 0.10$ (\bullet).

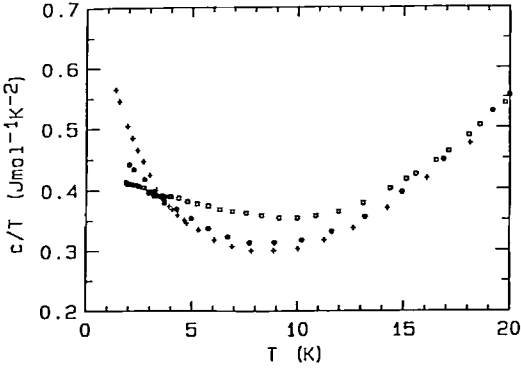


Fig. 5. High-field specific-heat data of UPt_3 in a plot of c/T vs. T for a field direction perpendicular to the hexagonal axis (a -axis); $B = 0$ T (\square), $B = 20$ T ($+$), $B = 24.5$ T (\bullet).

order does not destroy the heavy-fermion state. In order to analyse the specific heat of UPt_3 , different approaches have been followed. The following expression has frequently been used:

$$c/T = \gamma^* + \beta^* T^2 + \delta T^2 \ln T,$$

with $\beta^* = \beta - \delta \ln T^*$, where β is the usual phonon coefficient, T^* a characteristic temperature and δ the coefficient of the $T^3 \ln T$ term. For palladium concentrations between 1 and 10 at%, an additional peak occurs in the specific heat and eq. (1) is certainly not applicable in the temperature range where this peak is apparent. In another type of analysis, the heavy-fermion part in the specific heat has been separated from the total specific heat by applying Grüneisen relations [17,18]. The entropy involved with the heavy-fermion contribution of UPt_3 almost exactly approaches a value of $R \ln 2$ near room temperature. The heavy-fermion contribution resembles in some respects a spin 1/2 Kondo-type of contribution, although there are clear-cut differences. Guided by the knowledge of the values for the Grüneisen parameters in UPt_3 , the same method has been applied to $U(\text{Pt}_{0.95}\text{Pd}_{0.05})_3$. Here, the additional contribution arising from the long-range antiferromagnetic order has to be separated as well, making the analysis extremely complex. Nevertheless, above the ordering temperature the heavy-fermion contribution can still be regarded as a Kondo-type of specific-heat contribution with $T_K = 6.8$ K instead of 22 K as found for pure UPt_3 . The Grüneisen analysis is essentially a combined analysis of specific-heat and thermal-expansion data, preferentially of the same sample. Thermal expansion data for the $U(\text{Pt}_{0.90}\text{Pd}_{0.10})_3$ sample are not yet available and for this compound a further quantitative analysis has to be postponed. At this moment, we restrict ourselves to the observation that the γ^* value

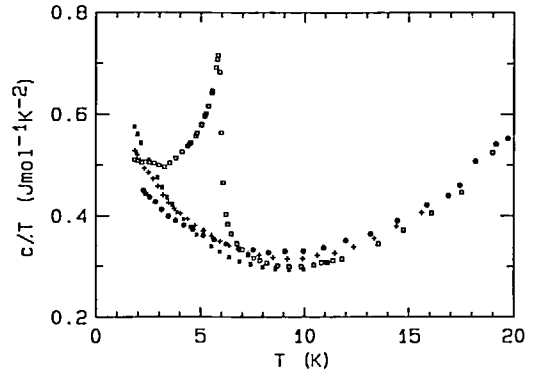
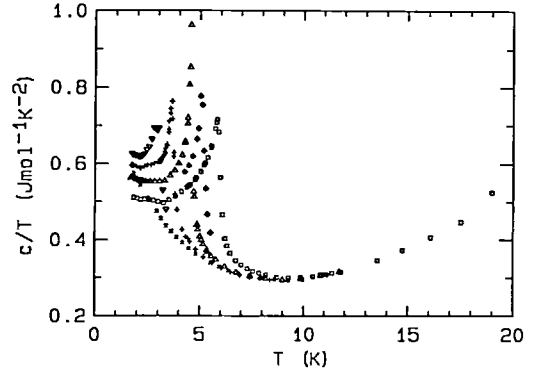


Fig. 6. (Upper panel) high-field specific-heat data of $U(\text{Pt}_{0.95}\text{Pd}_{0.05})_3$ in a plot of c/T vs. T for a field direction perpendicular to the hexagonal axis (b -axis); $B = 0$ T (\square), $B = 6$ T (\blacklozenge), $B = 8$ T (\triangle), $B = 10$ T ($+$), $B = 11$ T (∇), $B = 12$ T (\times). (Lower panel) high-field specific-heat data of $U(\text{Pt}_{0.95}\text{Pd}_{0.05})_3$ in a plot of c/T vs. T for a field direction perpendicular to the hexagonal axis (b -axis); $B = 0$ T (\square), $B = 12$ T (\times), $B = 16$ T ($+$), $B = 20$ T (\bullet).

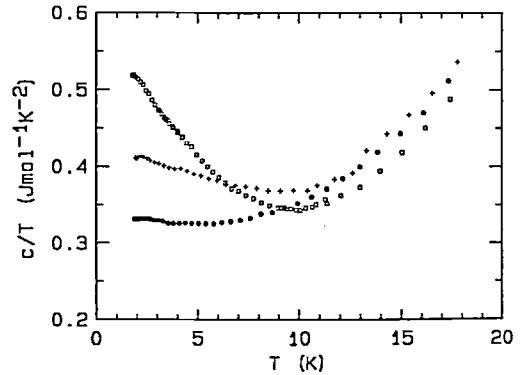


Fig. 7. High-field specific-heat data of $U(\text{Pt}_{0.90}\text{Pd}_{0.10})_3$ in a plot of c/T vs. T for a field direction perpendicular to the hexagonal axis (b -axis); $B = 0$ T (\square), $B = 10$ T ($+$), $B = 20$ T (\bullet).

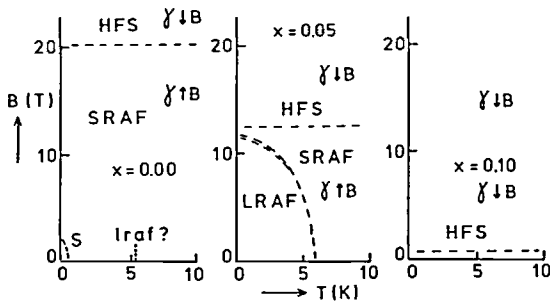


Fig. 8. Schematic phase diagram of different $U(\text{Pt}_{1-x}\text{Pd}_x)_3$ compounds; HFS: heavy-fermion state; S: superconducting state; SRAF: state with short-range antiferromagnetic correlations; LRAF: long-range antiferromagnetically ordered state with magnetic moments of about $0.6\mu_B$ per uranium atom; lraf: long-range antiferromagnetically ordered state with extremely small magnetic moments of $0.02\mu_B$ per uranium atom (not in all samples observable); the field effect on the specific heat is indicated.

for $U(\text{Pt}_{0.90}\text{Pd}_{0.10})_3$ is enhanced with respect to that of pure UPt_3 . Consequently, the characteristic temperature of $U(\text{Pt}_{0.90}\text{Pd}_{0.10})_3$ is reduced with respect of that of UPt_3 and reaches an approximate value of 10 K.

The field effect on the specific heat of the three $U(\text{Pt}, \text{Pd})_3$ samples is presented in figs. 5–7. Experiments are shown for the field applied along the a -axis and b -axis in the hexagonal plane. The results for UPt_3 have been discussed before: the low-temperature specific heat increases with magnetic field until the field reaches a value of 20 T; above 20 T the c/T values at the lowest temperatures start to decrease. This particular field effect has been discussed in terms of short-range antiferromagnetic correlations that are suppressed above the metamagnetic transition at 20 T. The data for the 5 at% Pd alloy show a more complex picture because of the long-range antiferromagnetic order that is largely depressed by magnetic fields up to 12 T. In the 12 T specific-heat curve, the transition is not visible anymore. Instead, we observe above 12 T for the 5 at% Pd alloy the same features as found for pure UPt_3 above 20 T: a depression of the c/T values at the lowest temperatures with increasing field values. There is a striking overall resemblance between the specific-heat curves of $U(\text{Pt}_{0.95}\text{Pd}_{0.05})_3$ in fields above the metamagnetic transition field and the specific-heat curves of pure UPt_3 above 20 T shown in fig 5. This resemblance can be extended to the 10 at% Pd specific-heat results as well: the c/T curve of $U(\text{Pt}_{0.90}\text{Pd}_{0.10})_3$ in zero field is very much alike the c/T curve of $U(\text{Pt}_{0.95}\text{Pd}_{0.05})_3$ in 12 T. A similar analogy was also observed in magnetization experiments: the same maximal value for the differential susceptibility perpendicular to the c -axis of about

$400 \times 10^{-9} \text{ m}^3/\text{mol}$ is found in UPt_3 near 20 T, in $U(\text{Pt}_{0.95}\text{Pd}_{0.05})_3$ near 11 T and in $U(\text{Pt}_{0.90}\text{Pd}_{0.10})_3$ at zero field. The above discussion is schematically represented by fig. 8 where the phase diagrams in the B - T plane for the three different $U(\text{Pt}, \text{Pd})_3$ compounds are compared at field directions perpendicular to the hexagonal axis. For the $x = 0.05$ compound, the two phase lines between the LRAF and SRAF states refer to the results for fields applied along the a - and b -axis in the hexagonal plane [19]. It should be noted that for fields applied along the hexagonal axis hardly any effect on the LRAF and SRAF states has been observed in specific-heat measurements [16,20]. In that case the phase boundary between the superconducting and SRAF or lraf states is also different with larger values for $-\partial B_{c2}/\partial T$ near T_c for fields applied along the hexagonal axis. In fact the phase diagram in the superconducting state is a multicomponent one resulting in a double peak in the specific heat at the transition to the superconducting state [21]. It is a challenging question whether the multicomponent phase diagram is related to the weak antiferromagnetism in the lraf state that is observed in some UPt_3 samples below 5 K.

Part of this work has been supported by the “Stichting Fundamenteel Onderzoek der Materie” (FOM) with financial support from the “Nederlandse Organisatie van Wetenschappelijk Onderzoek” (NWO). The work of A.d.V. is supported by the “Koninklijke Nederlandse Academie van Wetenschappen” (KNAW).

References

- [1] P.H. Frings, J.J.M. Franse, F.R. de Boer and A. Menovsky, *J. Magn. Magn. Mat.* 31–34 (1983) 240.
- [2] J.J.M. Franse, *J. Magn. Magn. Mat.* 31–34 (1983) 819.
- [3] A. de Visser, J.C.P. Klaasse, M. van Sprang, J.J.M. Franse, A. Menovsky, T.T.M. Palstra and A.J. Dirkmaat, *Phys. Lett. A* 113 (1986) 489.
- [4] A. de Visser, J.C.P. Klaasse, M. van Sprang, J.J.M. Franse, A. Menovsky and T.T.M. Palstra, *J. Magn. Magn. Mat.* 54–57 (1986) 375.
- [5] B. Batlogg, D.J. Bishop, E. Bucher, B. Golding, Jr., A. Ramirez, Z. Fisk, J.L. Smith and H.R. Ott, *J. Magn. Magn. Mat.* 63 & 64 (1987) 441.
- [6] A.P. Ramirez, B. Batlogg, E. Bucher and A.S. Cooper, *Phys. Rev. Lett.* 57 (1986) 1072.
- [7] G.R. Stewart, A.L. Giorgi, J.O. Willis and J. O'Rourke, *Phys. Rev. B* 34 (1986) 4629.
- [8] J.J.M. Franse, K. Kadowaki, A. Menovsky, M. van Sprang and A. de Visser, *J. Appl. Phys.* 61 (1987) 3380.
- [9] P.H. Frings, B. Renker and C. Vettier, *J. Magn. Magn. Mat.* 63 & 64 (1987) 202.
- [10] R. Verhoef, A. de Visser, A. Menovsky, A.J. Riemersma and J.J.M. Franse, *Physica B* 142 (1986) 11.
- [11] J.J.M. Franse, M. van Sprang, A. de Visser and A.A. Menovsky, *Physica B* 163 (1990) 511.

- [12] K. Kadowaki, M. van Sprang, J.C.P. Klaasse, A.A. Menovsky, J.J.M. Franse and S.B. Woods, *Physica B* 148 (1987) 22.
- [13] G. Aeppli, A.I. Goldman, G. Shirane, E. Bucher and M.Ch. Lux-Steiner, *Phys. Rev. Lett.* 58 (1987) 808.
- [14] P.H. Frings, B. Renker and C. Vettier, *Physica B* 151 (1988) 499.
- [15] H.P. van der Meulen, Z. Tarnawski, J.J.M. Franse, J.A.A.J. Perenboom, D. Althof and H. van Kempen, *Physica B* 163 (1990) 385.
- [16] H.P. van der Meulen, Z. Tarnawski, A. de Visser, J.J.M. Franse, J.A.A.J. Perenboom, D. Althof and H. van Kempen, *Phys. Rev. B* 41 (1990) 9352.
- [17] J.J.M. Franse, M. van Sprang, E. Louis, K. Kadowaki and A. de Visser, *J. Magn. Magn. Mat.* 76 & 77 (1988) 147.
- [18] J.J.M. Franse, M. van Sprang, A. de Visser and P.E. Brommer, *Physica B* 154 (1989) 379.
- [19] A. de Visser, M. van Sprang, A.A. Menovsky and J.J.M. Franse, *J. de Phys.* 49 (1988) C8-761.
- [20] M. van Sprang, R.A. Boer, A.A. Menovsky and J.J.M. Franse, *Japan. Appl. Phys.* 26 (1987) S26-3 563.
- [21] R.A. Fisher, S. Kim, B.W. Woodfield, N.E. Philips, L. Taillefer, K. Hasselbach, J. Flouquet, A.L. Giorgi and J.L. Smith, *Phys. Rev. Lett.* 62 (1989) 1411.